CHAPTER IV
PREPARATION AND CHARACTERIZATION OF POLYPYRROLE-LAYERED SILICATE NANOCOMPOSITES

ABSTRACT

Polypyrrole (PPy) was synthesized in the presence of octadecylammonium-montmorillonite (OC-MMT) 1-9 wt% using ferric chloride as an initiator. XRD results revealed that among these compositions, intercalated nanocomposites of OC-MMT and PPy were generated with a significant amount of expanded Na-MMT remaining in the mixture. TGA results showed that the PPy had much improved in thermal resistance with a higher degradation temperature and lower weight loss compared to pure PPy. By FTIR, it was revealed that the materials prepared were intercalated nanocomposites with both OC-MMT and unmodified Na-MMT. After doping PPyC3 with DBSA, XRD patterns showed that the doped one was the nanocomposites containing intercalated OC-MMT and exfoliated Na-MMT. It has better thermal resistance than undoped ones. The conductivity of the nanocomposites in ambient condition increased with OC-MMT content. Doping is less efficient to enhance conductivity in the presence of OC-MMT. Resistance and response time to CO_2, CH_4 and C_2H_4 increased with sample thickness. PPyC9 and DPPyC3 showed the lowest resistance to CO_2 and only PPyC9 to C_2H_4 while all samples except nDPPyC3 showed the lowest resistance to CH_4. From cross sensitivity, it was found that these samples are good sensors but not selective for these gases.

Keywords

Polypyrrole; Nanocomposites; Octadecylammonium-monymorillonite

INTRODUCTION

Electrically conductive polymers have been vigorously investigated over the last two decades. The development of research on these polymers has been growing due to their outstanding properties and wide applications. Conducting polymers have been utilized in many fields, such as biological technologies [1], electronic devices [2-3], batteries [4], and sensors [5]. Today, protection of the environment and persons is more important than before. For this reason, there is a need for improved or new sensors for measuring both physical and chemical changes. Nowadays, there is a great interest in making conductive polymer sensors. Selampinar *et al.* [5] found that several organic materials have been shown to exhibit resistivity changes when exposed to various gases.

Among the numerous electrically conductive polymers, polypyrrole (PPy) has often been studied due to its high conductivity, good chemical and environmental stability, and ease of preparation. Conducting PPy can be obtained in various forms, e.g. films or powders. They can also be produced by several techniques, including chemical polymerization and electrochemical polymerization; however, limitations of PPy in their properties, such as weak mechanical properties and poor thermal stability have to be improved in order to achieve satisfactory applications. There are several research works on the preparation and characterization of electrically conductive polypyrrole in order to improve its shortcomings and to achieve the satisfactory applications [6-7]. Bhat *et al.* [8] revealed that the PVDF/PPy films prepared by electrochemical polymerization of pyrrole on a very thin PVDF matrix film showed a decrease in tensile strength as the PPy content decreased, while the conductivity remained more or less similar to that of pure PPy. Jesus *et al.* [9] also prepared electrically conductive nanocomposites by a selective in situ polymerization of pyrrole within the lamellae ionomeric microdomains of sulfonated poly(styrene-*b*-(ethylene-*alt*-propylene)), SEP, diblock copolymers. They reported that incorporation of PPy into the block copolymer did not affect the alternating lamellae microstructure of the block copolymer but helped to improve the modulus of the melt above T_g of the sulfonated

polystyrene microdomains. Moreover, a conductivity of 10^{-3}-10^{-1} S/cm was achieved parallel to the film surface for PPy concentrations from 5-11 wt% of PPy.

Nanocomposites, comprised of glass fibers and other inorganic materials and some polymer, have been studied extensively. In these reinforced composites, the polymer and additives are not homogeneously dispersed on a nanometer level. If nanometer dispersion could be achieved, the mechanical properties might be further improved. A clay mineral is a potential nanoscale additive because it comprises silicate layers in which the fundamental unit is 1 nm thick planar structure. On the basis of clay crystalline properties, silicate clays can be divided into three major groups, which are kaolinite, montmorillonite (MMT), and hydrous micas groups [10]. Among these three groups of silicate layers, MMT has often been used because of its nano-thickness sheet allowing intercalation properties [11-13]. MMT is a hydrous alumina silicate mineral with counterions present between the clay layers whose lamellae are constructed from an octahedral alumina sheet sandwiched between two tetrahedral silica sheets. It has been shown that most of the properties are enhanced in the presence of a small amount of clay [14-20]. The nanocomposites may be prepared either by a blending process, melt blending or solution blending. Hong *et al.* [21] employed the direct one-step emulsion polymerization method to synthesize polypyrrole-montmorillonite nanocomposites by using DBSA as emulsifier and dopant. From the XRD patterns and the TEM photographs, they found the intercalation of PPy-DBSA between the clay layers in nanoscale. Moreover, the results from TGA showed that the thermal stability of PPy-DBSA/clay samples was improved due to the introduction of the clay. Furthermore, polypyrrole/caprolactam-modified montmorillonite clay composite was electropolymerized on a gold substrate by Liu *et al.* [22]. From the TGA results, it was clearly shown that the electropolymerized PPy/caprolactam-modified clay composite became more stable because at the ending temperature of 800°C, the weight loss of pure PPy reached 73.2% while that of the composite was just 44.0%. In addition, the SEM micrographs revealed

that the obtained film appeared to be more densely packed for the PPy/caprolactam-modified clay composites; in contrast, pure PPy film showed a rougher and more porous surface morphology. Moreover, the conductivity of the composites was significantly enhanced from 26.4 S/cm for pure PPy to 322 S/cm and it could depress aging in comparison to pure PPy.

In this work, attempts were made to prepare octadecylamine modified clay (OC-MMT), polypyrrole and its nanocomposites by an oxidation polymerization process in the presence of organically modified clay with and without doping agent, dodecylbenzenesulfonic acid sodium salt (DBSA). Compared with electrosynthesis, chemical polymerization has an advantage in large-scale production and cost economy, therefore, oxidative polymerization was preferred. The characteristics of the prepared nanocomposites were elucidated by x-ray diffraction, thermogravimetric analysis, FT-IR, and conductivity measurement in the presence of CO_2, CH_4 and C_2H_4.

EXPERIMENTAL

Materials

Pyrrole of 97% purity was purchased from Merck and was purified by vacuum distillation and stored in a refrigerator at about 4°C before use. Iron (III) chloride $FeCl_3.6H_2O$, a product of Fluka, was used without further purification as an oxidizing agent. Sodium montmorillonite (Na-MMT) with cation exchange capacity of 119 meq/100g was supplied by Kunimine Industrial Co., Ltd., Japan. Dodecylbenzenesulfonic acid sodium salt, a product of Fluka, was used as a doping agent. Octadecylamine (OC) for modification of Na-MMT was obtained from Fluka.

Preparation of Organically Modified Montmorillonite (OC-MMT)

The octadecylammonium-montmorillonite (OC-MMT), an organically modified montmorillonite, was synthesized by an ion exchange reaction between Na-MMT and octadecylamine (OC). Na-MMT (10 g) was stirred in 300 mL distilled water for 2 hours and heated at 80°C for half an hour. A

solution of 1.5 equivalent of OC and 3 equivalent of HCl was heated at 80°C at the same time as Na-MMT suspension for half an hour to give an octadecylammonium solution. The alkylammonium solution was added with vigorous stirring to the Na-MMT suspension kept at 80°C. The reaction was left for 2 hours and then the OC-MMT was recovered by filtration, rinsed with 2 L of hot distilled water. The obtained product was dried overnight at 80°C, ground with a centrifugal ball mill, and was kept in a bottle [23].

Synthesis of Polypyrrole (PPy)

Polypyrrole was chemically synthesized in 50 mL distilled water by mixing a 0.043 mole (2.881g) of pyrrole solution with a 0.1 mole (27.03 g) of an oxidizing solution of $FeCl_3$ (molar ratio of $FeCl_3$/pyrrole = 2.3:1). The pyrrole solution was kept in the bath before adding $FeCl_3$ and the addition was carried out slowly at low temperature due to the highly exothermic reaction. The synthesis was allowed to proceed at 5-7°C for one hour. The precipitate polypyrrole was collected by filtration, rinsed with distilled water and dried in a vacuum oven at 35°C [24].

Preparation of PPy/OC-MMT Nanocomposites

Polypyrrole-layered silicate nanocomposites (PPyC) were synthesized by mixing 1, 3, 6, and 9% weight of OC-MMT with pyrrole at room temperature. The pyrrole/OC-MMT mixture was cooled in a bath with slow stirring at 5-7°C followed by slowly adding $FeCl_3$ solution. The synthesis was performed in one hour. The resulting product was collected by filtration, rinsed with distilled water and dried in a vacuum oven at 35°C.

Preparation of DBSA-doped PPy/OC-MMT Nanocomposites

DBSA-doped polypyrrole-layered silicate nanocomposite with 3 wt% of OC-MMT (DPPyC3) was prepared by stirring PPyC3 (3% by weight of OC-MMT) in a solution of DBSA for one hour. The DBSA solution was obtained by dissolving DBSA (7.4836 g) in 50 mL distilled water. The PPy:DBSA

mixture molar ratio of DPPyC3 was 1:0.5; H^+/PhN = 0.5 [25] while the molar ratio of nDPPyC3 was 1:1; H^+/PhN = 1 (14.9672 g of DBSA). At the end of the reaction, the product was collected by filtration, rinsed with distilled water and dried in a vacuum oven at 35°C. The compositions of PPy/OC-MMT nanocomposites were shown in Table 1.

Characterization of the Nanocomposites

After modification of Na-MMT, sodium ions in the galleries of MMT were replaced by the quarternary ammonium ions of octadecylamine, a modifying agent, and the organically modified MMT (OC-MMT) was characterized using FT-IR, XRD, and TGA. FT-IR was used to determine functional groups of organic substances. The spectra were obtained from a BRUKER Equinox 55 spectrometer, using 16 scans at a resolution of 4 cm^{-1}. A deuteriated triglycinesulfate detector (DTGS) with a specific detectivity, D*, of $1x10^9$ $cm.Hz^{1/2}.W^{-1}$ was used to measure intensities within the frequency range of 4000-400 cm^{-1}. KBr pellet technique was applied in the preparation of samples. XRD spectra were recorded using a D/MAX-2000 series of Rigaku/X-ray Diffractometer that provides X-ray radiation of Cu K-alpha at 40 kV/30 mA. The glass sample holders were employed for all the samples. The experiment was operated in the 2θ range of 2-30 degree at the scan speed of 5 degree/min and 0.02 degree of scan step. A DuPont TGA 2950 was employed to study the degradation temperature of the materials. The chamber was continuously flushed with both nitrogen gas and oxygen gas separately at the flow rate of 20 mL/min. The temperature range studied was between 30-800°C for a modifying agent and the clay, and was between room temperature to 650°C for pure PPy and the nanocomposites. The heating rate was set at 10°C/min. Electrical resistance of samples was measured using a Keithley Electrometer Model 6517. Under ambient air atmosphere, an AC voltage of 10 volt was applied for 60 seconds and the resulting resistance was then measured. For measuring resistance of samples under CO_2, CH_4, C_2H_4 atmosphere, the pressure of gas was set at 0.1-0.3 bars and an AC voltage was

applied at 10 volts. The mixed gas between CO_2+CH_4 and CO_2+C_2H_4 was also tested at different ratios of supplied pressure. The resulting resistance was then measured with time up to 300 seconds. The samples were prepared in the pellet form using Hydraulic Press, GRASEBY SPECAC (8 bars pressure for 2 min).

RESULTS AND DISCUSSION

Characterization of PPy/OC-MMT nanocomposites

FT-IR

The incorporation of PPy into the galleries of the clay could be confirmed by using FT-IR. Figure 1 showed the FT-IR spectra of OC-MMT, PPy, DBSA and PPy/OC-MMT nanocomposites at various wt% of OC-MMT. From Figure 1, the FT-IR spectra of pure PPy showed a broad absorption band of OH group at about 3400-3200 cm^{-1}. It also showed the band at 1550 cm^{-1} due to C=C backbone stretching. The characteristic bands of PPy were observed at around 1250 and 1080 cm^{-1} due to C-N and C-H in-plane vibrations, respectively. The characteristic IR absorption peaks of OC-MMT were found at about 2800 and 1040 cm^{-1} for the vibration of methylene and Si-O groups, respectively. All FT-IR spectra of the nanocomposites at various wt% of OC-MMT showed the characteristic peaks of both PPy and OC-MMT. This showed that there was no loss of OC from OC-MMT during the preparation of the nanocomposites. The FT-IR spectrum of the dopant DBSA showed the aliphatic C-H bands at 2916 and 2841 cm^{-1}. The characteristic peak of SO_3^- of DBSA was also seen around 1149 cm^{-1}. For DPPyC3, the FT-IR spectra showed the characteristic peaks of PPy, OC-MMT and a doping agent, DBSA. This result could confirm that PPyC3 was doped with DBSA.

XRD

The XRD spectra of pure PPy and the PPy/OC-MMT nanocomposites with various wt% of OC-MMT were shown in Figure 2. PPy showed an amorphous structure over 2-40 degrees of XRD. It could be clearly observed from Figure 2 that the XRD spectra of PPy/OC-MMT nanocomposites

prepared by chemical polymerization of pyrrole in the presence of 1, 3, 6, and 9 wt% of OC-MMT showed the shift in peak position of OC-MMT from around 3.38 degrees (26.12 Å) to 3.36-3.26 degrees (26.14-26.95 Å). There was a peak at 7.66-7.54 degrees (11.47-11.65 Å) corresponding to that of pristine Na-MMT (around 7.72 degrees or 11.44 Å) that may be unmodified and still remained in the prepared OC-MMT. The d-spacing was gradually expanded with increasing OC-MMT content in PPy and totally disappeared in DBSA-doped sample. The higher OC-MMT content, the broader the peak. These suggested that among these OC-MMT compositions, intercalated nanocomposite of OC-MMT and PPy was generated with more number of interrupted (expanded) Na-MMT. For DPPyC3, the slightly shift in peak position of OC-MMT to lower degree obviously occurred from 3.38 degrees (26.12 Å) to 3.28 degrees (26.78 Å) but there was no peak present in the position of the remaining Na-MMT. This indicated that the silicate layers of the remaining Na-MMT were separated into expanded layers and relatively far from each other, at least with the same dimension as those expanded OC-MMT. Thus, DBSA can further expand silicate layers of the OC-MMT and totally expand those unmodified MMT to get the nanocomposites containing intercalated OC-MMT and exfoliated Na-MMT instead of the mixture of expanded OC-MMT and unmodified MMT.

TGA

The values of DTGA, degradation temperature (T_d) at starting point, %moisture, and %residue of all the samples under N_2 and O_2 atmosphere up to 650°C were shown in Table 3a and 3b, respectively while the TGA thermograms were shown in Figure 3a and Figure 3b for N_2 and O_2 atmosphere up to 650°C, respectively. The degradation temperatures and the weight loss (%) of PPy/OC-MMT nanocomposites increased with the amount of OC-MMT while moisture absorption decreased in comparison to those of the pure PPy. The temperature at 10% weight loss for the pure PPy and all of the PPy/OC-MMT nanocomposites under N_2 and O_2 were around 180 and

290°C, respectively. At the ending temperature under N_2, the weight loss of all of the samples was not greater than 50% and not much different while the weight loss of pure polypyrrole under O_2 was much greater than that of the nanocomposites, suggesting that pure polypyrrole was much easier to be oxidized than the nanocomposites. As shown in Figure 3b, the degradation of the pure PPy was first observed at about 100°C due to moisture and the weight loss reached 82% at the end of 650°C. For PPy/OC-MMT nanocomposites with 1, 3, 6, and 9 wt% of OC-MMT, the obvious degradation began at about 300°C with two transitions. The first transition was rather fast followed by much slower degradation of the second transition. This was possibly due to the loss of OC molecules and some parts of PPy followed by further degradation of PPy. In the case of DPPyC3; however, it had better thermal resistance than the others. At the ending temperature of 650°C, the weight loss of all of the nanocomposites was greater than 40%. This could confirm that PPy in the form of PPy/OC-MMT nanocomposites had much improved thermal resistance when compared to that of the pure PPy.

Resistivity measurements

Electrical resistance of the obtained pure PPy and PPy/OC-MMT nanocomposites were determined by a Keithley Electrometer Model 6517. The plot of resistance under CO_2 atmosphere of pure PPy and PPyC3 of 0.5mm thick samples vs. time (raw data obtained from the electrometer) was shown in Figures 4 and 5, respectively. From these two curves, there was a marked decrease in resistance in the first 100 seconds and the first 90 seconds for PPy and PPyC3, respectively, followed by mostly constant resistance values up to 300 seconds. Time at the lowest resistance was defined as "response time" and electrical resistance reported in this work was resistance at the defined response time.

Resistivity under ambient air atmosphere

Electrical resistance of PPy/OC-MMT nanocomposites at various wt% of OC-MMT compared to that of pure PPy under ambient air atmosphere were shown in Figure 6. The pure PPy and the nanocomposites with 1-3 wt% OC-MMT give relatively similar resistance, 866.8 ohms. The resistance of PPy/OC-MMT nanocomposites reduced with further increase in the OC-MMT content. This suggested that the intercalation induced longer conjugation length to facilitate electron mobility, corresponding to the results from FTIR that the peaks positions of C=C backbone stretching being 1550 and 1514 cm^{-1} for pure PPy and the PPy/OC-MMT nanocomposites, respectively, indicating that the conjugation length of the latter was longer than the former [22]. For DPPyC3, it showed slightly reduced in resistance when compared to that of PPyC3 and its resistance was still higher than those of PPyC6 and PPyC9. This meant that DBSA doping in the presence of OC-MMT was less efficient to enhance the conductivity of PPy than the introduction of OC-MMT. This result was in contrast to the work of Hong *et al.* [21] who showed that by doping PPy with DBSA before mixing with montmorillonite, the nanocomposites showed higher conductivity. It may be due to the barrier effect by the interruption of clay layers to obstruct DBSA penetration to PPy molecules, so it was not convenient for DBSA to dope or oxidize polypyrrole to enhance conductivity. Moreover, from x-ray result, DBSA is probably undergone ion-exchange with sodium ion of the remaining pristine montmorillonite and thus less effective to dope PPy.

Resistivity under CO_2, CH_4 and C_2H_4

Response time to CO_2, CH_4 and C_2H_4 at room temperature for pure PPy and all the nanocomposite films of 0.5, 0.8 and 1.0mm thick at various wt% of OC-MMT was shown in Figures 7a, 7b and 7c, respectively. Among the three gases, ethylene gives the fastest response time despite that its molecular size is the largest. It was found that the films of 0.5mm thick showed the lowest response time (minimum at 60-90 sec). Moreover, response time to CO_2, CH_4 and C_2H_4 for all the sensor samples increased with the

sample thickness. For CO_2, increase in the OC-MMT content tends to render higher response time, especially when thickness increases. However, the response time of the 1 wt% OC-MMT/PPy nanocomposite is always lower than pure PPy. For methane, the nanocomposites also show faster response time than the pure one but the content of OC-MMT does not effect the response time for the thin piece but the thick ones tend to have longer response time with amount of OC-MMT. The doped one gives the fastest response time. For ethylene, the effect of OC-MMT content on response time is more or less like those of methane but at faster response. So, the thickness of 0.5 mm is probably the optimum one to avoid effect of OC-MMT content on the response time.

Figures 8a, 8b and 8c showed resistance at response time to CO_2, CH_4 and C_2H_4 for pure PPy and all the nanocomposite films of 0.5, 0.8 and 1.0mm thick, respectively. These figures revealed that at the thickness of 0.5mm, all the samples showed the lowest resistance compared to the sample films of 0.8 and 1.0mm. Among the three gases, methane shows the lowest resistance indicating that it is more effective to allow charge transfer in PPy than carbon dioxide and ethylene, respectively. Resistance to CO_2, CH_4 and C_2H_4 for pure PPy and all the nanocomposites increased with the thickness of sample films. For 0.5 mm thick specimens in CO_2, increasing OC-MMT content results in lower resistance or increasing conductivity; on the other hand, OC-MMT content is almost no influence on resistance in methane and ethylene atmospheres. The fluctuation of the resistance with increasing OC-MMT content is more obvious when thickness increases, probably in accordance to longer response time. DBSA gives a poor doping effect to reduce resistance (since an effective dopant usually enhances conductivity of certain conductive polymers by several orders of magnitude), i.e. just comparable to that of 6-9 wt% OC-MMT. DPPyC3 and PPyC9 showed the lowest resistance to CO_2 while PPyC1 and PPyC9 showed the lowest resistance to CH_4 and C_2H_4, respectively.

It is well known that PPy conductivity can be enhanced by acid/salt doping or by oxidation mechanism [26]. Among the four atmospheres, air and

CO_2 are oxidative while ethylene and methane are more reducing. In other words, both CH_4 and C_2H_4 are electron donating molecules that lower the carrier density, reflecting in the increase in resistance of PPy. Thus when the latter two gases contact to PPy, poorer conductivity could be expected. However, carbon dioxide may induce some oxidation to carbon atom in PPy such that effective conjugation length in PPy becomes less than those found in methane environment. So for pure gas, the PPy/OC-MMT nanocomposites is more likely sensitive to methane than the other two gases.

The results of resistance in air and CO_2, relatively oxidized atmospheres, suggest that PPy molecular chains that are intercalated in between clay galleries are elongated to allow easier path for electron movement and hop. The number of confined chains increases with the OC-MMT content so that conductivity increases with amount of OC-MMT. For ethylene gas having the largest molecular size, the resistance is the highest due to both reducing effect and the retardation of charge mobility. Thus the resistance in ethylene gas reaches to equilibrium (response time) faster than those in oxidative gases.

Effect of dopant concentration on response time and resistance to CO_2, CH_4 and C_2H_4 of DPPyC3 and nDPPyC3 films of 0.5mm thick were investigated as shown in Figures 9a and 9b. In the case of sensor to CO_2, CH_4 and C_2H_4, DPPyC3 showed slightly lower resistance with longer response time compared to those of nDPPyC3. The poorest conductivity was found again in ethylene than in methane and carbon dioxide. It is interesting that increasing concentration of doping agent does not effectively enhance the conductivity of PPy in the presence of OC-MMT. This was correspondent to the results obtained under ambient air condition that the presence of clay layers obstructed DBSA to form bonds with polypyrrole, resulting in poorly increase in the conductivity of polypyrrole. Therefore, it could be conclude that the DBSA is unsuccessful to function as an effective dopant for PPy/OC-MMT nanocomposites

Effect of gas concentration on resistance to CO_2, CH_4 and C_2H_4 are shown in Figure 10, 11 and 12, respectively for all samples at the gas pressure

of 0.1, 0.2 and 0.3 bars. From these three graphs, it was found that resistance of the samples increased with the gas pressure and reduced with OC-MMT content. The increase in resistance with the gas amount attributes to the reduction in number of charge carriers and obstacles for charge mobility by the adsorbed gas molecules [5]. Moreover, there was a linear relationship between the pressure of gas and resistance. These suggested that PPy and PPy/OC-MMT nanocomposites can be good sensors for these gases.

Resistivity under the mixed gases CO_2:CH_4 and CO_2:C_2H_4

Figures 13a and 13b showed response time and resistance at room temperature to CO_2:CH_4 at the ratio of gas pressure (bars) 1:1, 1:2 and 1:3 for all of the sensor samples, respectively. It was found that when increasing the pressure of CH_4, the response time was fluctuated within 40-80 s, especially at gas ratio of 1:3 (showing fastest response) and resistances of PPy and all the nanocomposite films increased. This is due to CH_4 is an electron donating molecule that causes a reduction in the charge carrier density of PPy, resulting in an increase in resistance [5]. It should be noted that, in the mixed gases system, the resistance increases with OC-MMT content for gas ratio 1:1 and becomes independent to OC-MMT content at high gas ratio. This indicates that methane can suppress the enhancement of conductivity by chain elongation at high OC-MMT content. The inversed conductivity dependent on OC-MMT content attributed to complex oxidative and reducing environment that makes more defects or deprotonated/protonated positions in the structure.

Response time and resistance to CO_2:C_2H_4 at the ratio of 1:1, 1:2 and 1:3 of PPy and all the nanocomposites of 0.5mm thick were also studied as shown in Figures 14a and 14b. Similar to CO_2:CH_4 mixed gases, the response time in CO_2:C_2H_4 is fluctuated within 60-100 s (slower than in CO_2:CH_4) and the response time is again shorter with high gas ratio while conductivity becomes worse. Ethylene is also effective to suppress conductivity dependent on OC-MMT content.

The cross sensitivity ratio of CO_2 to CH_4 and CO_2 to C_2H_4 in the mixture of CO_2:CH_4 and CO_2:C_2H_4 at the ratio of 1:1, 1:2 and 1:3 for all of the

sensor samples was shown in Table 4 and Table 5, respectively. Cross sensitivity of each gas was calculated from resistance of the sample to the gas mixture divided by resistance of that sample to each gas. Cross sensitivity of the sample to each pure gas in the gas mixture should be marked different and the sample, whose cross sensitivity is closer to 1, is selective for that gas. However, for these sets of gases their resistance values are in the same range and thus the cross sensitivity for either gas is not much different and closed to 1, see Tables 4-5. This meant that all of these samples were not selective to CO_2 and CH_4. Like the system of CO_2:CH_4, sensitivity of all samples to CO_2 and C_2H_4 was relatively similar as shown in Table 5, suggesting that they were also not selective to C_2H_4. In other words, the PPy/OC-MMT nanocomposites are good sensors for these gases but not selective to the mixed gaseswithin a response time of one minute at ambient condition.

CONCLUSIONS

In this study PPy/OC-MMT nanocomposites of 1-9 wt% OC-MMT were chemically synthesized. The nanocomposites prepared were the intercalated nanocomposites of OC-MMT and PPy with more number of expanded remaining Na-MMT but the one doping with DBSA was the combination of intercalated OC-MMT and exfoliated remaining Na-MMT nanocomposites. When using OC-MMT, PPy had much improved thermal resistance and moisture absorption (dependent on clay content) with higher degradation temperature and lower weight loss of 40% at 650°C while pure PPy had weight loss >80%. The obvious degradation of the nanocomposites was observed at about 300°C. The temperature at 10% weight loss of the pure PPy was around 180°C while that of the nanocomposites was about 290°C. With high loading of OC-MMT, the thermal behavior changed from one transition to two transitions; i.e. first fast degradation due to the loss of OC molecules and some parts of PPy followed by much slower second degradation due to further degradation of PPy. In the case of DPPyC3, however, it had better thermal resistance than the others with one transition. Moreover, the

conductivity of PPy under ambient air atmosphere was enhanced by adding OC-MMT. The higher the OC-MMT content, the higher the conductivity of the nanocomposites. Addition of OC-MMT was more efficient in increasing the conductivity of PPy in ambient air than DBSA doping in the PPy nanocomposite with OC-MMT.

Response time and electrical resistance of pure PPy and all the nanocomposite sensors to CO_2, CH_4, and C_2H_4 increased with an increase in the thickness of sample films. PPyC9 and DPPyC3 showed the lowest resistance to CO_2 and only PPyC9 to C_2H_4 while all samples except nDPPyC3 showed the lowest resistance to CH_4. The concentration of doping agent in the presence of clay did not affect the resistance of the nanocomposites. However, the doping contributed to enhance conductivity for the interested gases. For the mixtures of CO_2:CH_4 and CO_2:CH_4, resistance of pure PPy and all the nanocomposites increased with increasing pressure of CH_4 and C_2H_4. The cross sensitivity for either gas in the systems of CO_2:CH_4 and CO_2:C_2H_4 was not much different and closed to 1, suggesting that these samples are good sensors but not selective for these gases.

Acknowledgements

The authors were grateful to Postgraduate Education and Research Programs in Petroleum and Petrochemical Technology (PPT Consortium) for the partial scholarship and funding for the research work and MTEC for the research grant no. MT-S-45-POL-09-213-G.

REFERENCES

1. Zinger, B., and Miller, L.L., *Journal of American Chemical Society*, **106**, 6861-6863 (1984).
2. Cooper, G.P., and Vincent, B., *Journal of Physics D: Applied Physics*, **22**, 1580-1585 (1989).
3. Makhlouki, M., Morsi, M. Bonnet, A., Conan, A., Pron, A., and Lefrant, S., *Journal of Applied Polymer Science*, **44**(3), 443-446 (1992).
4. Chen, J.H., Huang, Z.P., Wang, D.Z., Yang, S.X., Li, W.Z., Wen, J.G., and Ren, Z.F., *Synthetic Metals*, **125**, 289-294 (2002).

5. Fatma, S., Levent T., Ural, A., Talat, Y., and Sesik, S., *Synthetic Metals*, **68**, 109-116 (1995).
6. Fatma, S., Ural, A., Tulay, Y., Attila, G., and Levent, T, *Journal of Polymer Science: Part A: Polymer Chemistry*, **35**, 3009-3016 (1997).
7. Omastowa, M., Pavlinec, J., Pionteck, J., Simon, F., and Konisa, S., *Polymer*, **39**(25), 6559-6566 (1998).
8. Bhat, N.V., Geetha, P., Pawde, S., and Nallathambi, R., *Journal of Applied Polymer Science*, **58**, 2251-2257 (1995).
9. Jesus, M.C., Weiss, R.A., and Hahn, S.F., *Macromolecules*, **31**, 2230-2235 (1998).
10. Pinnavaia, T.J. and Beall, G.W., *Polymer-clay Nanocomposites*, (pp. 97-149). London: John Wiley & Sons Ltd. (2000).
11. Tyan, H.L., Liu, Y.C., and Wei, K.H., *Chemistry Materials*, **11**, 1942-1947 (1999).
12. Zhu, J. Morgan, A.B., Lamelas, F.J., and Wilkie, C.A., *Chemistry Materials*, **13**, 3774-3780 (2001).
13. Sinharay, S. and Okamoto, M., *Progress Polymer Science*, **28**, 1539-1641 (2003).
14. Biswas, M., ans Sinharay, S., *Polymer*, **39**(25), 6423-6428 (1998).
15. Kim, B.H., Jung, J.H., Kim, J.W., Choi, H.J., and Joo, J., *Synthetic Metals*, **117**, 115-118 (2001).
16. Liang, L., Liu, J. and Gong, X., *Langmuir*, **16**, 9895-9899 (2000).
17. Messersmith, P.B., and Guannelis, E.P., *Journal of Polymer Science: Part A: Polymer Chemistry*, **33**, 1047-1057 (1995).
18. Sinharay, S., and Biswas, M., *Materials Research Bulletin*, **34**(8), 1187-1194 (1999).
19. Wu, Q., Xue, Z., Qi, Z., and Wang, F., *Polymer*, **41**, 2029-2032 (2000).
20. Yeh, J.M., Liou, S.J., Lai, C.Y., and Wu, P.C., *Chemistry Materials*, **13**, 1131-1136 (2001).
21. Hong, S.H., Kim, B.H., Joo, J., Kim, J.W., and Choi, H.J., *Current Applied Physics*, **1**, 447-450 (2001).
22. Liu, Y.C. and Tsai, C.J., *Chemistry Materials*, **15**, 320-326 (2003).

23. Ratanarat, K., Nithitanakul, M., Martin, D.C., and Magaraphan, R., *Reviews on Advanced Materials Science*, **5**(3), 187-192 (2003).

24. Ramelow, U., Ma, J.H., and Darbeau, R., *Material Resolution Innovat*, **5**, 40-49 (2001).

25. Moon, G.H., and Seung, S.I., *Journal of Applied Polymer Science*, **71**, 2169-2178 (1999).

26. Kang, E.T., Neoh, K.G., and Tan, K.L, *Advances in Polymer Science 106 Polymer Characteristics*, (pp. 135-190). Berlin: Springer-Verlag (1993).

Table 1 Compositions of PPy/OC-MMT nanocomposites.

Sample	Pyrrole (g)	OC-MMT (g)	wt% OC-MMT	DBSA (g)
PPyC1[a]	2.8881	0.0291	1	-
PPyC3	2.8881	0.0891	3	-
PPyC6	2.8881	0.1389	6	-
PPyC9	2.8881	0.2849	9	-
DPPyC3	2.8881	0.0891	3	7.4836
nDPPyC3	2.8881	0.0891	3	14.9672

[a]Number at the end of acronym indicates weight% of OC-MMT in the nanocomposites.

Table 2 The basal spacing of Na-MMT, and OC-MMT.

MMT	Basal spacing (Å)
Na-MMT	12.41
OC-MMT	26.12

Table 3a The values of DTGA, T_d at starting point, %moisture, and %residue of all the samples under N_2 atmosphere up to 650°C.

Sample	DTGA	T_d at starting point	% moisture	% residue
PPy	255.21	215.85	6.47	48.84
PPyC1	298.59	275.00	1.72	67.74
PPyC3	285.00	248.25	1.96	64.19
PPyC6	291.17	243.17	1.79	62.74
PPyC9	280.11	241.11	1.48	61.15
DPPyC3	372.25	250.09	1.96	72.19

Table 3b The values of DTGA, T_d at starting point, %moisture, and %residue of all the samples under O_2 atmosphere up to 650°C.

Sample	DTGA	T_d at starting point	% moisture	% residue
PPy	269.73	235.15	7.16	16.04
PPyC1	322.58	254.12	1.97	55.31
PPyC3	318.94	250.00	1.16	60.44
PPyC6	315.26	247.98	0.83	61.30
PPyC9	300.09	266.47	1.61	59.87
DPPyC3	362.16	283.26	2.35	63.40

Table 4 Cross sensitivity ratios of CO_2 to CH_4 in the gas mixture of CO_2 and CH_4 at room temperature for all the sensor samples.

Sample	Cross sensitivity ratio		
	Ratio of gas		
	1:1	1:2	1:3
	CO_2:CH_4	CO_2:CH_4	CO_2:CH_4
PPy	0.99:1.00	1.01:1.02	1.01:1.02
PPyC1	1.00:1.01	1.01:1.02	1.02:1.02
PPyC3	1.00:1.01	1.01:1.02	1.02:1.02
PPyC6	1.00:1.01	1.02:1.02	1.02:1.02
PPyC9	1.01:1.01	1.02:1.02	1.02:1.02
DPPyC3	1.01:1.01	1.02:1.02	1.02:1.02
nDPPyC3	1.00:1.00	1.01:1.01	1.01:1.01

Table 5 Cross sensitivity ratios of CO_2 to C_2H_4 in the gas mixture of CO_2 and C_2H_4 at room temperature for all the sensor samples.

Sample	Cross sensitivity ratio		
	Ratio of gas		
	1:1	1:2	1:3
	CO_2:C_2H_4	CO_2:C_2H_4	CO_2:C_2H_4
PPy	0.99:0.99	1.01:1.01	1.01:1.01
PPyC1	1.00:0.99	1.01:1.01	1.01:1.01
PPyC3	1.01:1.00	1.02:1.01	1.02:1.01
PPyC6	1.01:1.00	1.02:1.01	1.02:1.01
PPyC9	1.02:1.01	1.02:1.01	1.02:1.02
DPPyC3	1.02:1.01	1.03:1.01	1.02:1.01
nDPPyC3	1.01:1.01	1.01:1.02	1.01:1.01

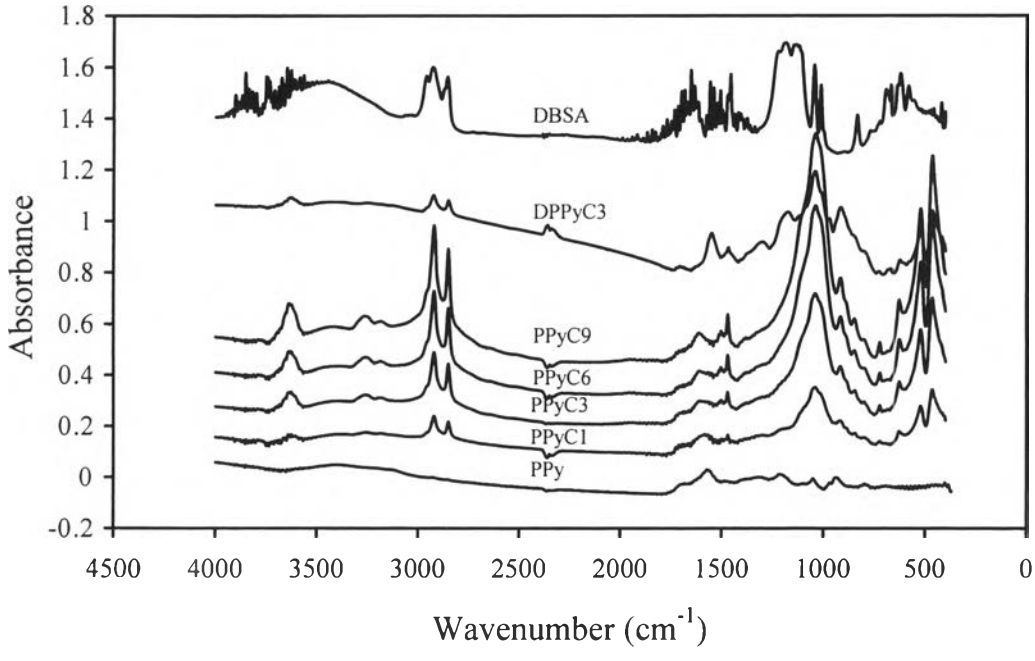

Figure 1 FT-IR spectra of OC-MMT, PPy, DBSA and PPy/OC-MMT nanocomposites at various wt% of OC-MMT.

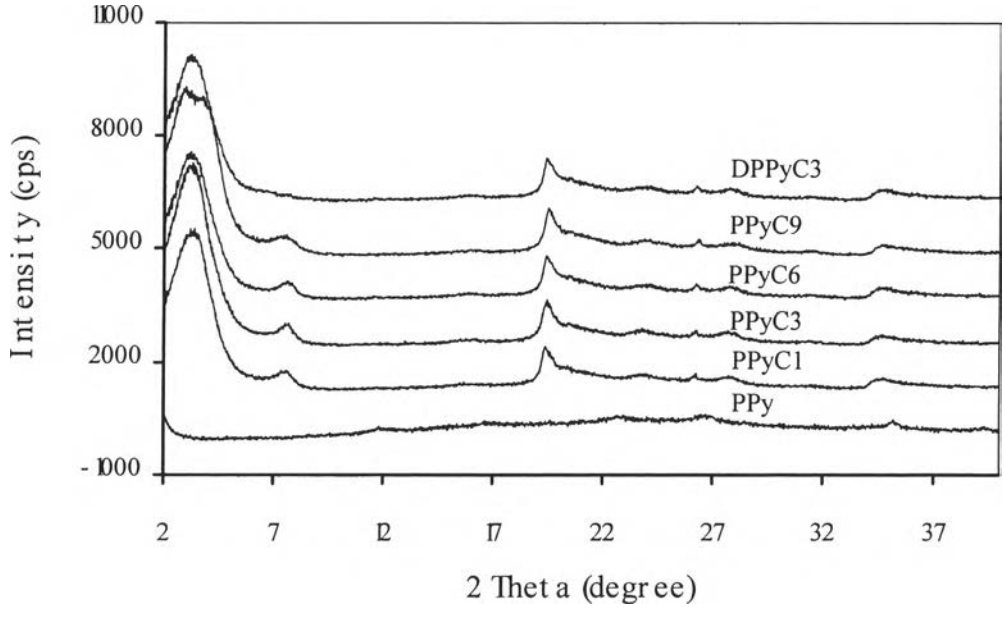

Figure 2 XRD patterns of pure PPy and PPy/OC-MMT nanocomposites at various wt% of OC-MMT.

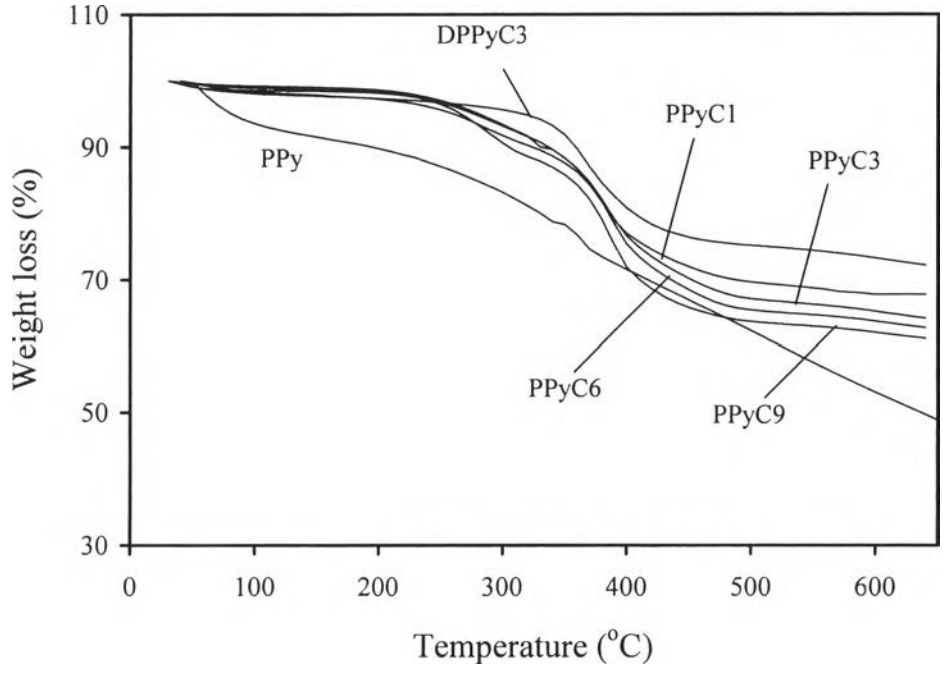

Figure 3a TGA curves of pure PPy and PPy/OC-MMT nanocomposites at various wt% of OC-MMT under N_2 atmosphere.

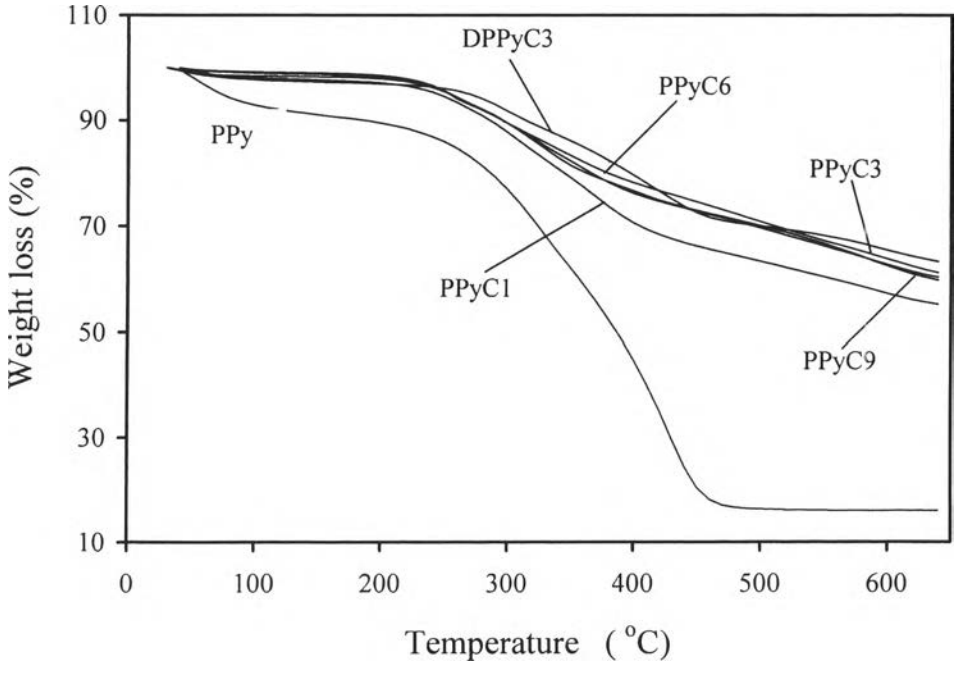

Figure 3b TGA curves of pure PPy and PPy/OC-MMT nanocomposites at various wt% of OC-MMT under O_2 atmosphere.

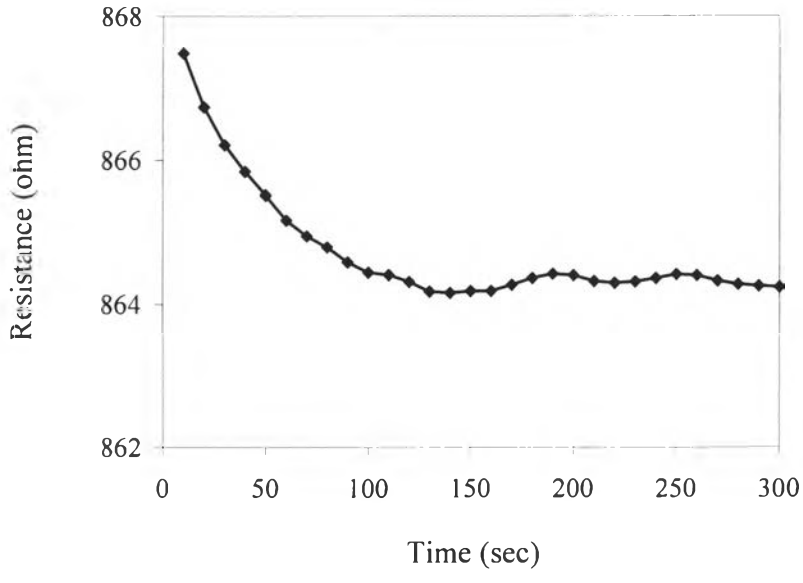

Figure 4 Resistance to CO_2 at room temperature at various times for pure PPy of 0.5mm thick.

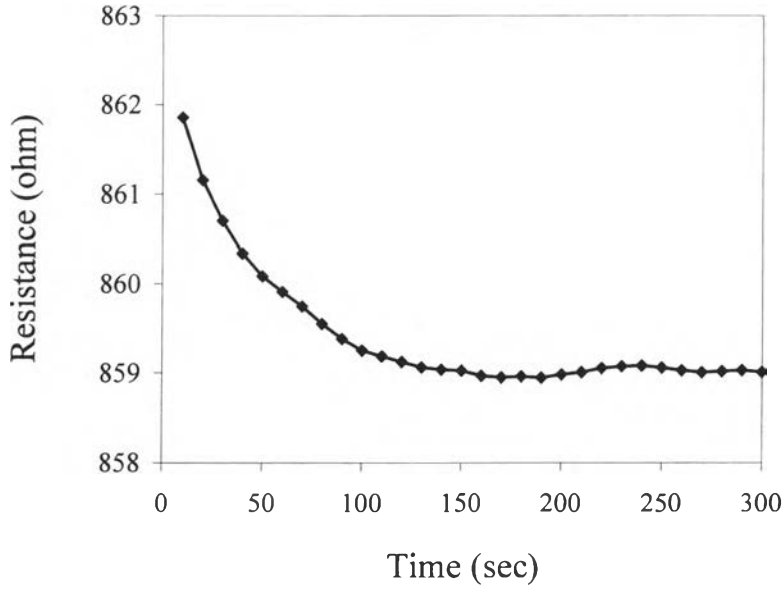

Figure 5 Resistance to CO_2 at room temperature at various times for PPyC3 of 0.5mm thick.

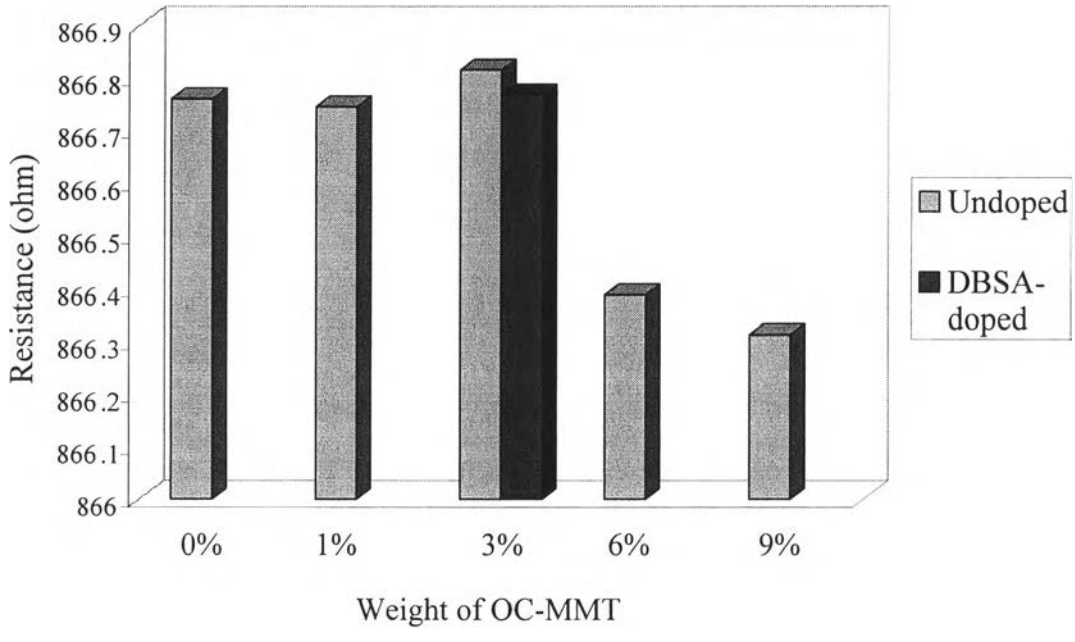

Figure 6 Resistance versus wt% of OC-MMT in the nanocomposites (1 mm thickness) under ambient air atmosphere measured after 60 seconds.

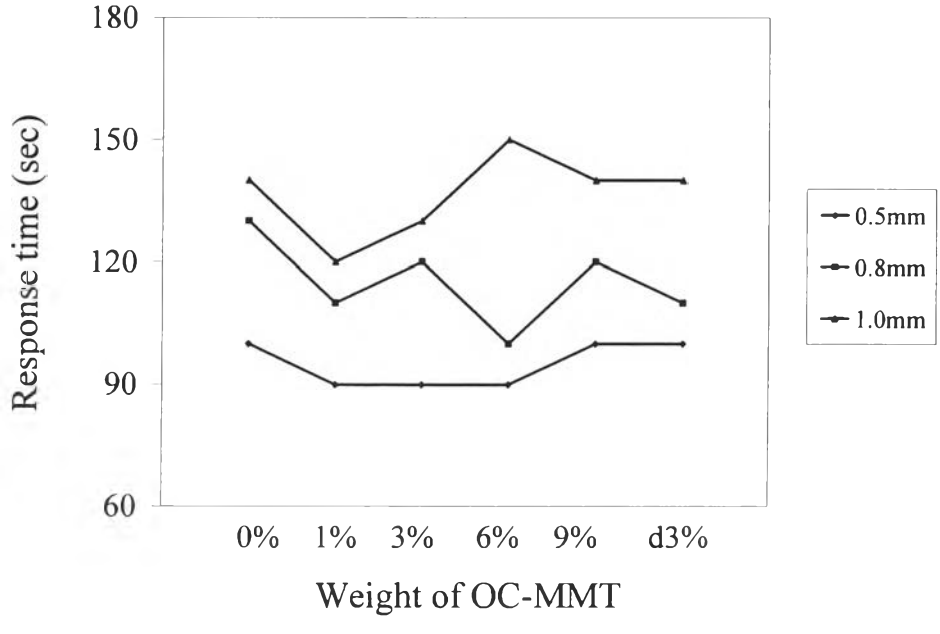

Figure 7a Effect of thickness on response time to CO_2 at room temperature for PPy and all of the nanocomposites.

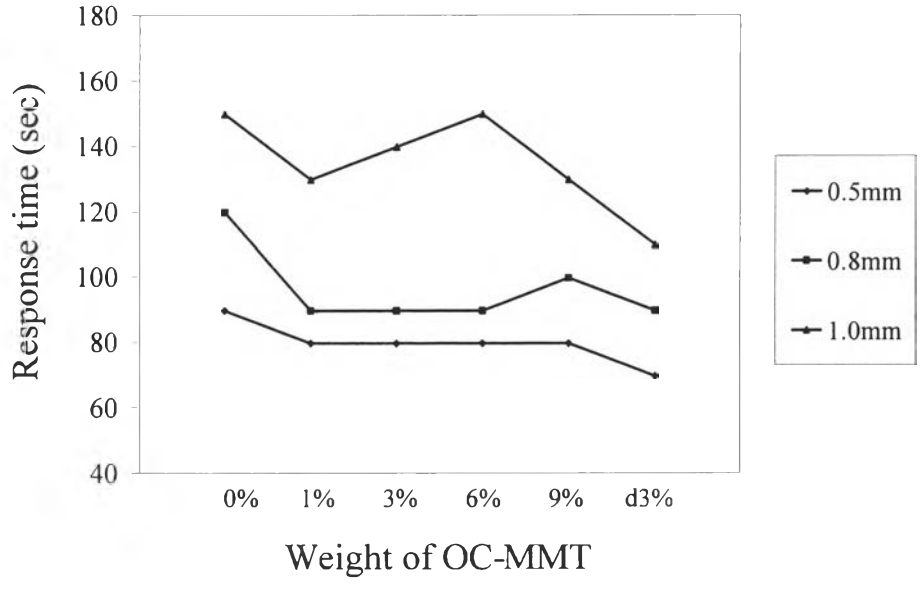

Figure 7b Effect of thickness on response time to CH_4 at room temperature for PPy and all of the nanocomposites.

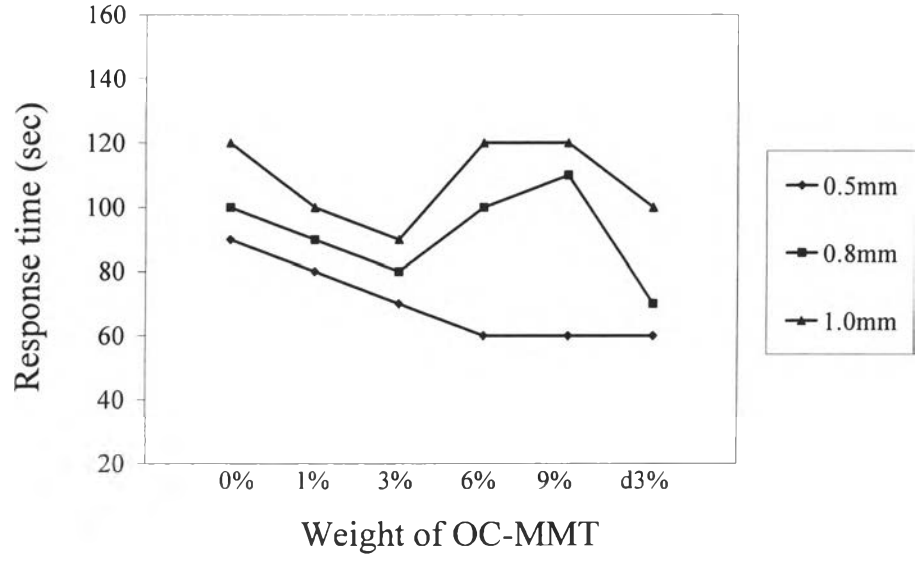

Figure 7c Effect of thickness on response time to C_2H_4 at room temperature for PPy and all of the nanocomposites.

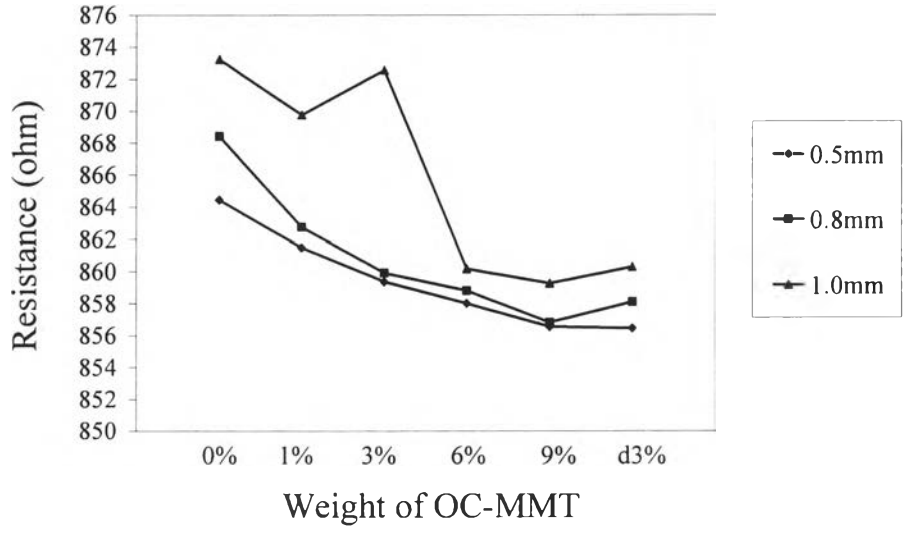

Figure 8a Effect of thickness on resistance to CO_2 at response time (room temperature) for PPy and all of the nanocomposites.

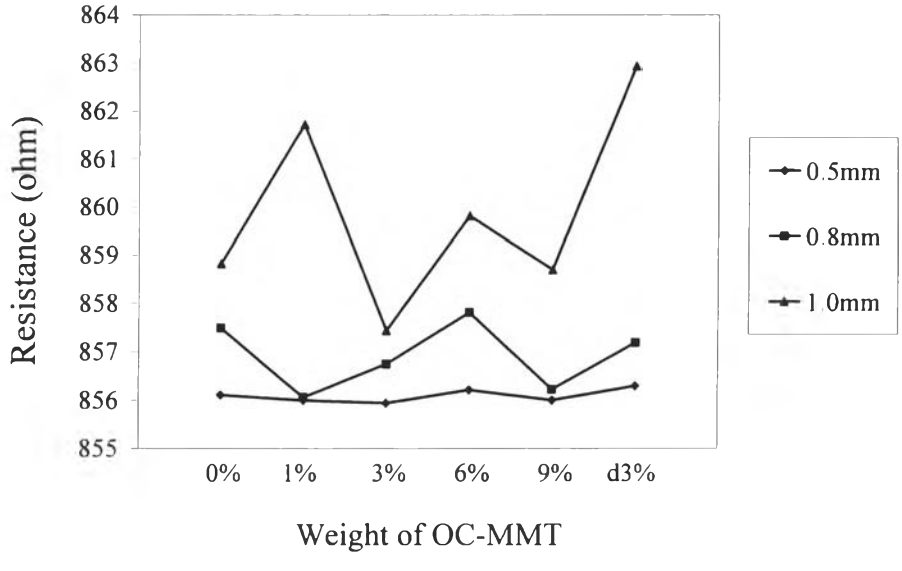

Figure 8b Effect of thickness on resistance to CH_4 at response time (room temperature) for PPy and all of the nanocomposites.

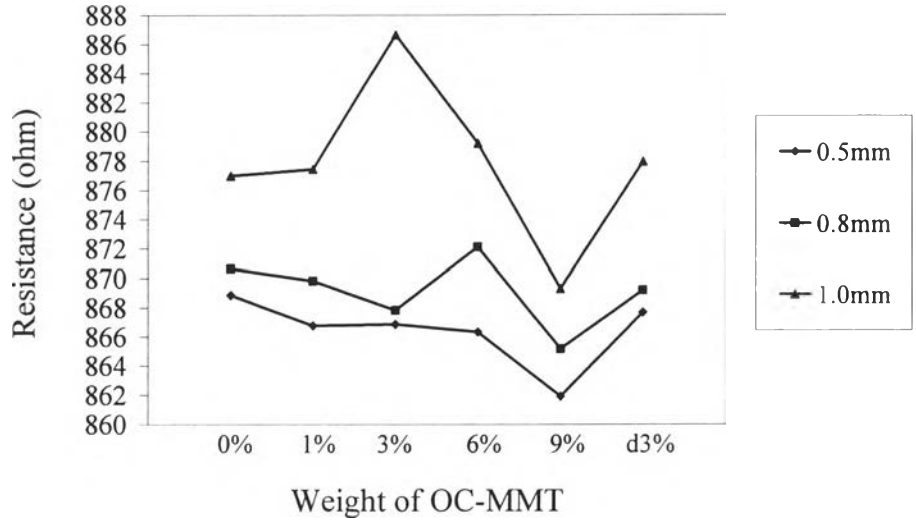

Figure 8c Effect of thickness on resistance to C_2H_4 at response time (room temperature) for PPy and all of the nanocomposites.

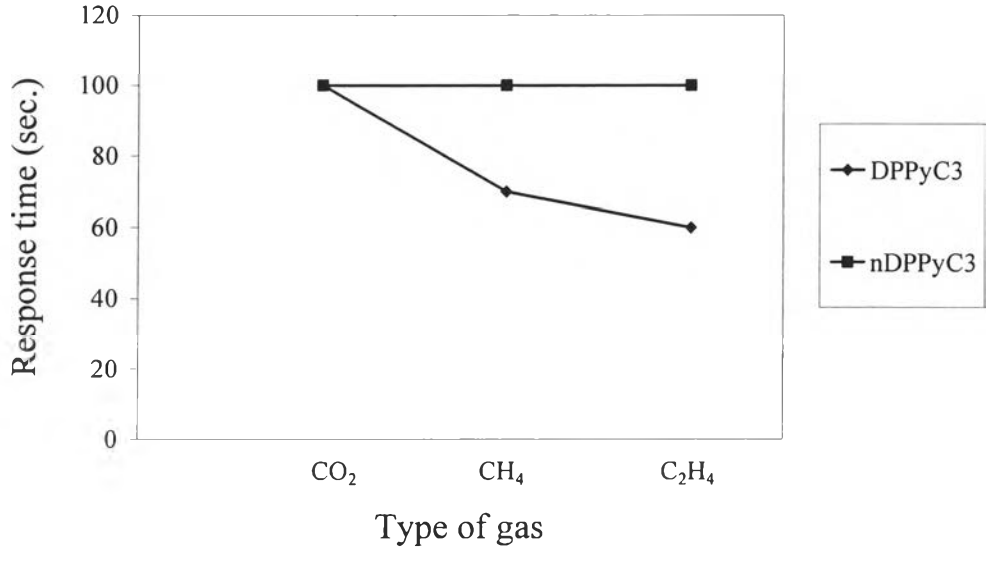

Figure 9a Response time to CO_2, CH_4 and C_2H_4 at room temperature for DPPyC3 and nDPPyC3 of 0.5mm thick.

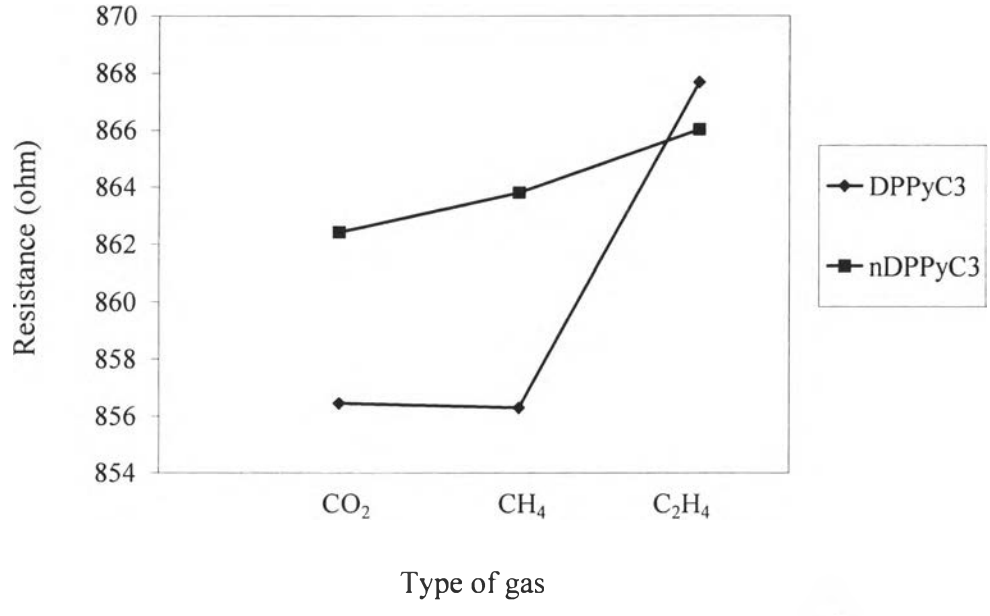

Figure 9b Resistance to CO_2, CH_4 and CH_4 at response time (room temperature) for DPPyC3 and nDPPyC3 of 0.5mm thick.

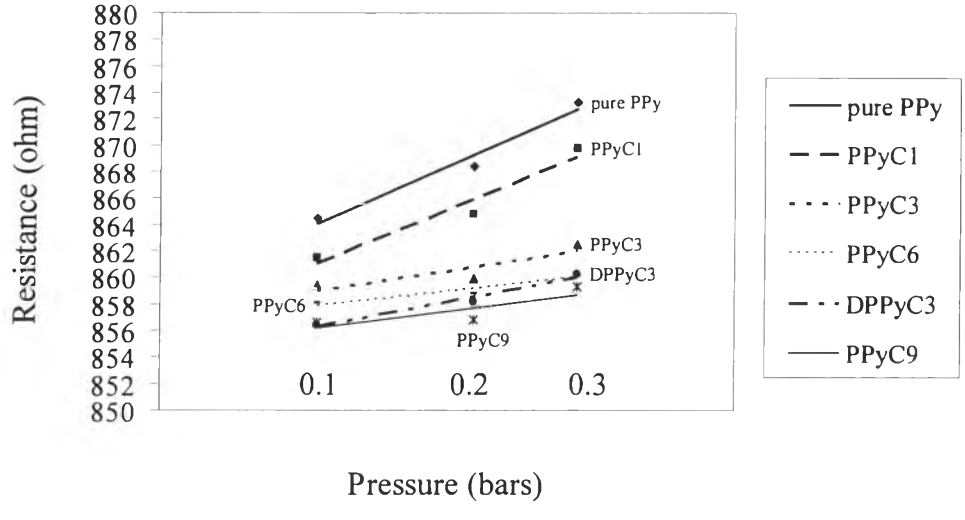

Figure 10 Resistance to CO_2 at the gas pressure of 0.1, 0.2 and 0.3 bars for all samples of 0.5mm thick.

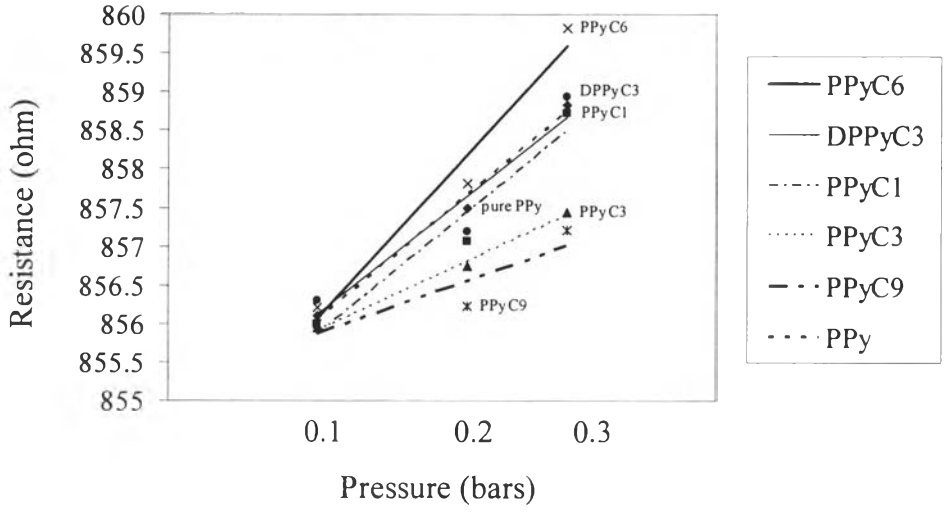

Figure 11 Resistance to CH_4 at the gas pressure of 0.1, 0.2 and 0.3 bars for all samples of 0.5mm thick.

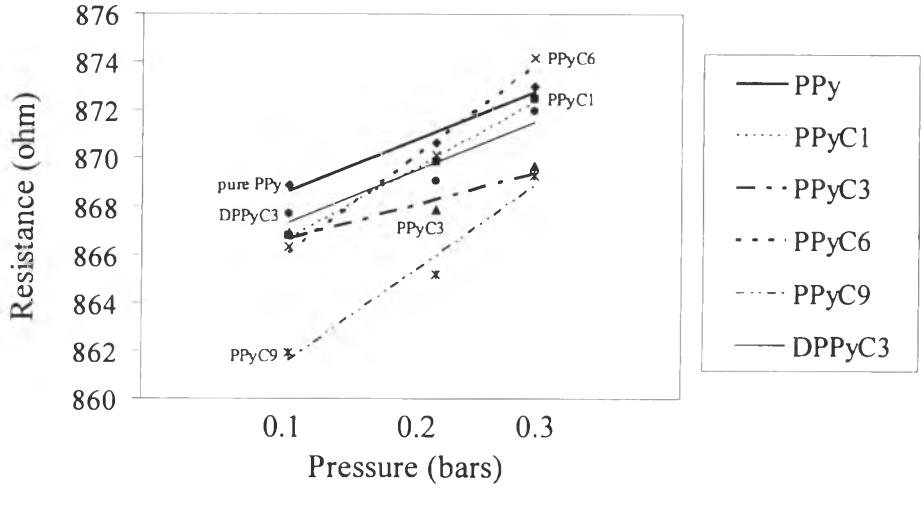

Figure 12 Resistance to C_2H_4 at the gas pressure of 0.1, 0.2 and 0.3 bars for all samples of 0.5mm thick.

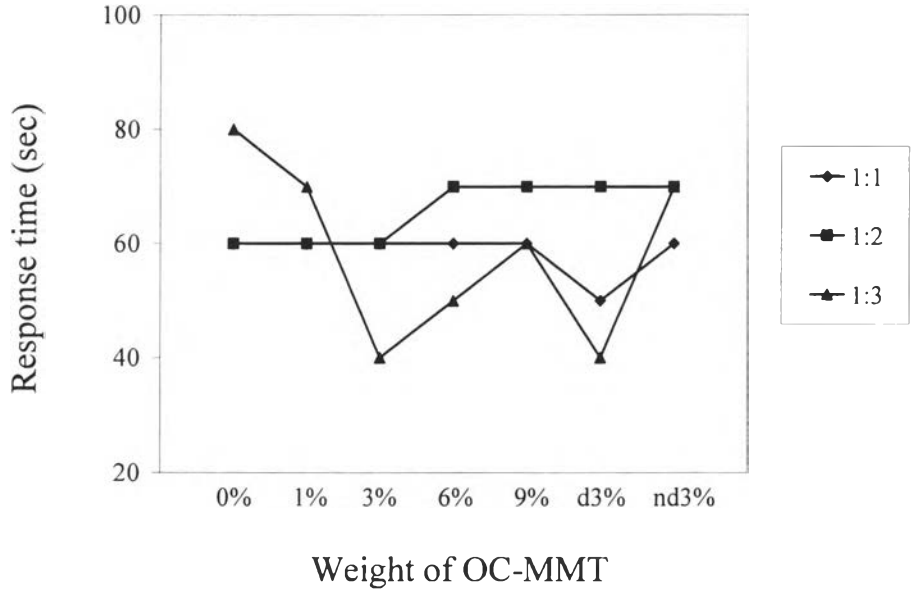

Figure 13a Response time to CO_2:CH_4 at the ratio of 1:1, 1:2 and1:3 at room temperature for PPy and all of the nanocomposites.

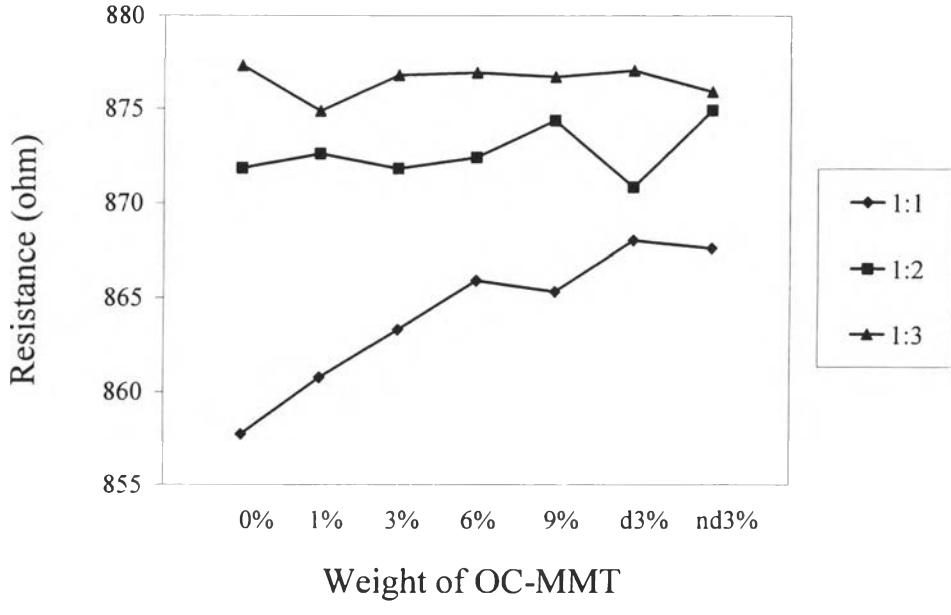

Figure 13b Resistance to CO_2:CH_4 at the ratio of 1:1, 1:2 and 1:3 at response time (room temperature) for PPy and all of the nanocomposites.

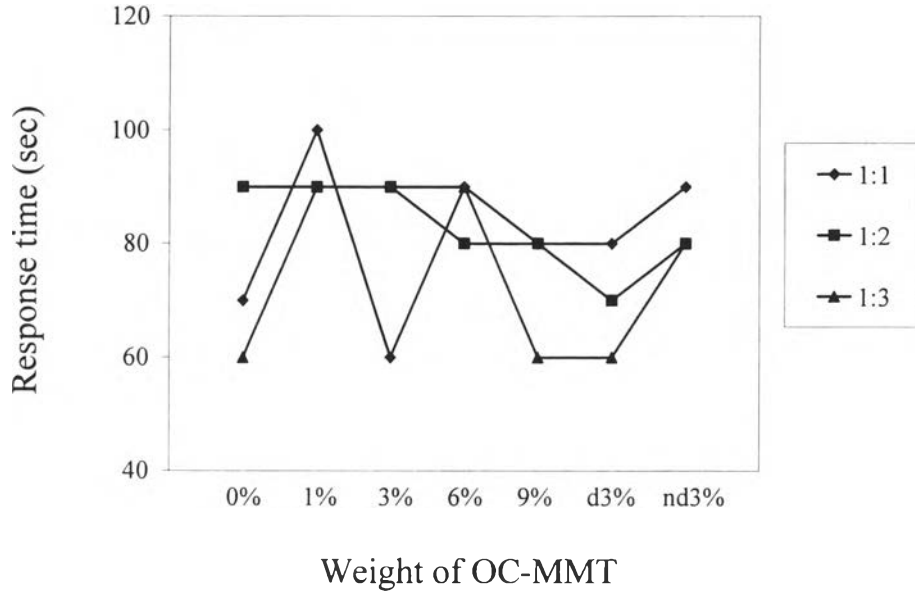

Figure 14a Response time to CO_2:C_2H_4 at the ratio of 1:1, 1:2 and 1:3 at room temperature for PPy and all of the nanocomposites.

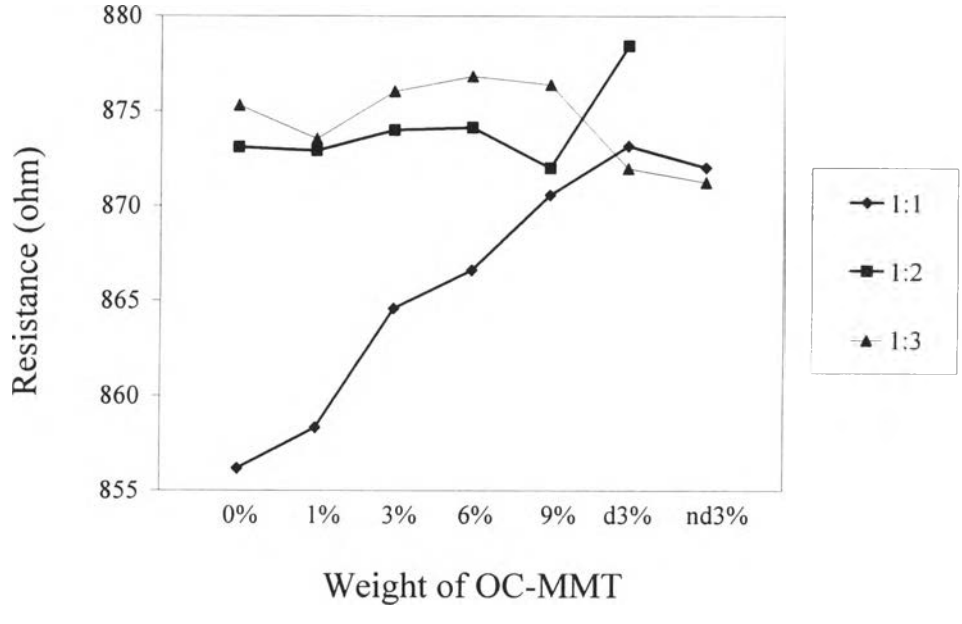

Figure 14b Resistance to CO_2:C_2H_4 at the ratio of 1:1, 1:2 and 1:3 at response time (room temperature) for PPy and all of the nanocomposites.